Author Manuscript

Author Manuscript

Author Manuscript

Author Manuscript

HHS Public Access

Author manuscript

Nanoscale. Author manuscript; available in PMC 2016 October 28.

Published in final edited form as:

Nanoscale. 2015 October 28; 7(40): 16571–16577. doi:10.1039/c5nr03411f.

Hybrid Upconversion Nanomaterials for Optogenetic Neuronal Control

Shreyas Shah[†], **Jingjing Liu**[‡], **Nicholas Pasquale**[†], **Jinping Lai**[†], **Heather McGowan**[‡], **Zhiping P. Pang**[‡,*], and **Ki-Bum Lee**[†,*]

[†]Department of Chemistry & Chemical Biology, Rutgers, The State University of New Jersey, Piscataway, NJ, U.S.A

[‡]Child Health Institute of New Jersey and Department of Neuroscience and Cell Biology, Rutgers-Robert Wood Johnson Medical School, New Brunswick, NJ, U.S.A

Abstract

Nanotechnology-based approaches offer the chemical control required to develop precision tools suitable for applications in neuroscience. We report a novel approach employing hybrid upconversion nanomaterials, combined with the photoresponsive ion channel channelrhodopsin-2 (ChR2), to achieve near infrared light (NIR)-mediated optogenetic control of neuronal activity. Current optogenetic methodologies rely on using visible light (e.g. 470-nm blue light), which tends to exhibit high scattering and low tissue penetration, to activate ChR2. In contrast, our approach enables the use of 980-nm NIR light, which addresses the short-comings of visible light as an excitation source. This was facilitated by embedding upconversion nanomaterials, which can convert NIR light to blue luminescence, into polymeric scaffolds. These hybrid nanomaterial scaffolds allowed for NIR-mediated neuronal stimulation, with comparable efficiency as that of 470-nm blue light. Our platform was optimized for NIR-mediated optogenetic control by balancing multiple physicochemical properties of the nanomaterial (e.g. size, morphology, structure, emission spectra, concentration), thus providing an early demonstration of rationally-designing nanomaterial-based strategies for advanced neural applications.

GRAPHICAL ABSTRACT

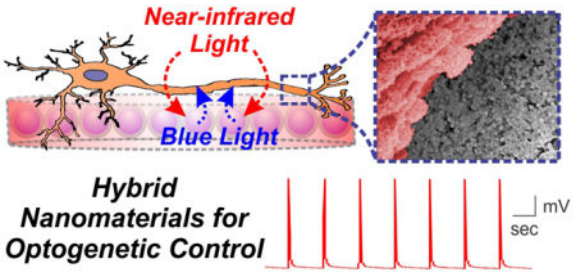

Upconverting nanomaterial-based hybrid scaffolds were employed to optogenetically stimulate neurons with near-infrared light.

*Correspondence: Prof. Ki-Bum Lee, Tel: 848-445-2081, Fax: 732-445-5312, kblee@rutgers.edu, http://kblee.rutgers.edu/. Prof. Zhiping P. Pang, Tel: 732-235-8074, Fax: 732-235-8612, pangzh@rwjms.rutgers.edu.

Author Manuscript Author Manuscript Author Manuscript Author Manuscript

The mammalian brain is a phenomenal piece of 'organic machinery', consisting of an intricate network of neurons dispersed in a mixture of chemical and biochemical constituents. While remarkable advances have been made to better understand the brain, the intrinsic complexity of the brain makes it difficult to probe the innate neuronal connectivity and to further modulate this activity. This is partly due to challenges in developing tools to effectively interact with the type of neurocircuitry found in the brain. Yet, given that the biomolecular interactions and chemical communication in the brain occur at the nanoscale, there is great interest in leveraging advances in nanotechnology for neuroscience research.[1] The reproducible control of chemical reactions and advanced nanoscience have enabled the generation of numerous types of nanomaterials and nanostructures with well-defined compositions, shapes and properties. This offers tremendous promise for creating a seamless integration of neural cells with synthetic materials, which can be further exploited to achieve improved control of neuronal activity and function. In this way, nanotechnology-based methods can be rationally-designed to interface with neural systems and to address prevalent challenges in neuroscience.

Herein, we demonstrate a unique application of inorganic-organic hybrid nanomaterials to the field of optogenetics. Optogenetics is a revolutionary technology that has transformed the field of neuroscience, allowing for the optical control of neuronal activity by using light ("opto") and genetically-encoded photosensitive proteins ("genetics").[2, 3] In the last decade, optogenetic approaches have been successfully utilized to explore numerous neural states and disorders including fear, anxiety, addiction, reward-seeking behavior, autism and Parkinson's disease.[4] While it has facilitated novel investigations that were previously infeasible, the efficient optogenetic manipulation of neural activity is contingent on delivering a sufficient dose of light to the target neuronal cells.[5] Visible light (~400–600 nm) has been primarily used in this regard to stimulate the photoresponsive opsin proteins (e.g. channelrhodopsins, ChR, that are activated by 470-nm blue light). A number of groups have also attempted to achieve optogenetic control using other wavelengths of illumination such as red-shifted light sources (>600 nm),[6, 7] which can offer opportunities for multiplexed stimulation. The most common approach to implement this strategy has involved the combination of genome-wide screening and complex molecular engineering to generate new variants of microbial opsin that are sensitive to red light.[8] However, such a strategy tends to require balancing numerous opsin-dependent design considerations including spectral specificity, optimal expression in target cells, efficient cellular trafficking to the plasma membrane and optimal kinetics/ion specificity.[9] While valuable, developing optogenetic approaches employing highly red-shifted light has proven to be technically challenging.

In this work, we have developed an upconversion nanomaterial-based system to act as a mediator for facilitating optogenetic control using near-infrared (NIR) light (980 nm). Upconversion nanoparticles (UCNPs) have attracted significant biomedical interest due to their inherent ability to emit high-energy visible light upon excitation with low-energy NIR light.[10] UCNPs possess a number of favorable characteristics compared to conventional fluorescent materials including high resistance to photoblinking and photobleaching, longer luminescence lifetimes and high signal-to-noise ratio due to weak background autofluorescence.[11] Moreover, by carefully controlling the experimental conditions during

Author Manuscript Author Manuscript Author Manuscript Author Manuscript

the synthesis process, the physicochemical properties of UCNPs (e.g. size, emission spectra, surface chemistry) can be finely-tuned based on the application of interest.[12] So far, these features have made UCNPs particularly ideal for numerous bio-applications including cellular labeling, imaging and drug delivery.[13–15] By generating a neural-material interface using UCNP-embedded polymer hybrid scaffolds, we provide one of the first demonstrations of upconversion nanomaterials as NIR-excitable internal light sources to achieve optogenetic control of mammalian neuronal activity (Fig. 1).

Acquiring optogenetic control of neurons relies on the exogenous expression of light-sensitive ion channels within the neuronal plasma membrane.[16] Channelrhodopsin-2 (ChR2) is one example of a microbial ion channel that conducts cation influx upon blue light illumination (~470–475 nm).[17] The stable expression of ChR2 in mammalian neurons can thus render the neurons sensitive to activation with blue light.[2] Given that the blue light-responsive ChR2 is well-established and widely-used in optogenetics, we sought to design UCNPs that can activate ChR2 upon NIR illumination. The upconversion process (from NIR light to visible light) in UCNPs is permitted by the doping of trivalent lanthanide ions within a host matrix.[10] Among other synthetic variables, selecting the proper lanthanide dopants is a critical factor that determines the wavelength-specific luminescence spectrum of the UCNP.[18] To this end, a combination of the lanthanide ions Yb^{3+} (a sensitizer, which has an absorption cross-section in the NIR spectral region) and Tm^{3+} (an activator, which has optical emission in the blue spectral region) is reported to be a suitable pair to achieve blue emission (~475 nm).[19, 20] We selected to employ Yb^{3+}/Tm^{3+}-doping for our study, since the resulting upconverted blue emission overlaps with the excitation spectra of ChR2,[21] thus suggesting the possibility for UCNP-mediated optogenetic activation.

We sought to synthesize monodispersed UCNPs that exhibit strong upconversion luminescence under NIR illumination. To this end, we synthesized β-hexagonal-phase UCNPs consisting of a sodium yttrium fluoride ($NaYF_4$) host matrix co-doped with Yb^{3+}/Tm^{3+} using a co-precipitation method from a previous report.[22] With modifications to the experimental conditions and further optimization, we synthesized $NaYF_4$: Yb^{3+}/Tm^{3+} UCNPs with 30 mol% Yb^{3+} and 0.2 mol% Tm^{3+}. Transmission electron microscopy (TEM) shows a spherical morphology of the particles, with an average diameter of 36.2 ± 1.5 nm (Fig. 2a). In order to preserve the optical integrity of the nanoparticles, we further coated the nanoparticles with an inert thin-shell of $NaYF_4$. This is reported to be an important step because lanthanide dopants exposed on the nanoparticle surface can undergo deactivation due to surface defects, lattice strains and interactions with the surrounding solvents.[23, 24] An inert shell can thus minimize surface quenching-induced emission loss and preserve high UCNP luminescence.[25] The epitaxial growth of a $NaYF_4$ shell was carried on the UCNP cores as reported previously.[24] TEM confirmed the shell formation and the monodisperity of the resulting core-shell UCNPs, which displayed an average diameter of 46.7 ± 2.4 nm (Fig. 2a). The core-shell UCNPs exhibited an absorption peak at 980 nm (Fig. S1 in ESI) and peak emission in the blue spectral region at ~475 nm upon excitation with 980-nm NIR light (Fig. 2b–c). Powder X-ray diffraction (PXRD) patterns exhibit peak positions and intensities that can be indexed with the β-hexagonal phase $NaYF_4$ crystal structure,[26] further confirming the high crystallinity of the UCNPs (Fig. 2d). The quantum yield of our core-shell UCNPs is expected to be ~1–3%, based on previous reports.[27, 28]

Author Manuscript Author Manuscript Author Manuscript Author Manuscript

With the as-synthesized core-shell UCNPs exhibiting favorable spectral properties for ChR2 activation, we next encapsulated the particles within a biomaterial scaffold. Biomaterials are becoming increasingly useful for neural engineering since they can be tailored to interact with nervous tissue on a molecular, cellular and tissue level.[29] At the same time, biomaterials can serve as reliable scaffolds to load and immobilize cells, biomolecules and other materials over long periods of time. To this end, compared to a solution-based delivery of UCNPs that can suffer from diffusion of particles over time and high variability in particle distribution, we elected to embed the UCNPs within a biomaterial scaffold for our studies. We used poly(lactic-co-glycolic acid) (PLGA) as the underlying biomaterial scaffold, since it is biocompatible, biodegradable, FDA-approved and widely-used for *in vivo* transplantation in the nervous system.[30, 31] In order to acquire a uniform nanoparticle distribution within the polymer matrix, UCNPs from a stock solution were first mixed with the PLGA solution. After thorough mixing to disperse the UCNPs, the PLGA-UCNP solution was spin-coated to form thin films on circular glass coverslips (Fig. 3a). A number of parameters were optimized including the amount of UCNP loading, percentage of PLGA and speed of spin-coating (see Supporting Information for details). Flexible thin films (~0.5 μm thickness) of PLGA-UCNP were generated that could be peeled from the glass coverslip (Fig. 3b). Moreover, the hybrid scaffolds showed blue luminescence under NIR irradiation, owing to the distribution of UCNPs throughout the polymer film (Fig. 3b). This luminescence spectra of the hybrid scaffold was evaluated using fluorescence emission spectroscopy (Fig. S2 in ESI), which confirmed the optical integrity and presence of UCNPs within the polymer films. Increasing the power of NIR illumination was further observed to exponentially increase blue light emission from the scaffolds, exhibiting a linear relationship on a double logarithmic scale (Fig. S3 in ESI). Further varying the initial amount of UCNPs mixed with the PLGA solution (prior to spin-coating) enabled the generation of films with varying concentrations of embedded UCNPs (quantification shown in Table S1), which were characterized using scanning electron microscopy (SEM) (Fig. S4 in ESI) and atomic force microscopy (AFM) (Fig. S5 in ESI). By tuning both the concentration of UCNPs embedded within the film and the power of NIR illumination, a range of blue emission output can be achieved (Fig. S6 in ESI).

The polymer-UCNP hybrid scaffolds were then utilized to achieve optical activation of cultured neurons expressing ChR2. Mouse hippocampal neurons were isolated from postnatal day 0 (P0) mice pups and plated on the hybrid scaffold surface pre-coated with Matrigel. Thereafter, the neuronal cultures were transduced with ChR2-tdTomato via lentiviruses after 4–5 days *in vitro* (DIV) growth. The neurons attached and showed complex morphology with extensive dendritic branching by 14 DIV (Fig. S7 in ESI). Cell viability assay further confirmed that the hybrid scaffold did not have any adverse effects on neuronal survival (Fig. S8 in ESI). SEM images display neurons cultured on the polymer scaffold with uniformly distributed UCNPs, thus allowing high localization of UCNPs in close cellular proximity (Fig. 3c).

At 14–15 DIV, we conducted whole-cell patch clamping experiments to measure the light-mediated neuronal response. The whole-cell patch clamp technique is a method to record the ionic current flow across the neuronal membrane, as well as changes in the membrane potential, in response to an applied stimuli (e.g. light).[32] Since ChR2 is a light-gated cation

Author Manuscript Author Manuscript Author Manuscript Author Manuscript

channel, the opening of this channel upon light illumination would facilitate the influx of cations and lead to an inward current flow to drive neuronal depolarization.[2, 17] The membrane-localized expression of ChR2 was first confirmed by the presence of tdTomato fluorescence using confocal microscopy (Fig. 4a). Not surprisingly, the inward current response could be induced in these cells when light-emitting diode (LED)-generated 470-nm light was supplied via the microscope objectives (Fig. 4b). We then delivered 980-nm NIR light using an external optical cable setup (Fig. S9 in ESI). Remarkably, an inward current response was immediately evident upon NIR light illumination, similar as that observed by using the conventional 470-nm light (Fig. 4b).

While the presence of an inward current flow is an indicator of successful UCNP-mediated optogenetic control, the generation of nerve impulses (i.e. action potentials) would provide stronger and more reliable functional evidence for our approach. Nerve impulses mediate the information flow in the nervous system, and can only be generated by a sufficient increase (i.e. depolarization) in the membrane potential past a predefined threshold.[33] Given that the time course of upconversion in UCNPs is less than half a millisecond (Fig. S10 in ESI), we were able to apply low NIR pulse widths that are generally used for optogenetic studies. In our studies, we checked for nerve impulse generation by applying brief pulses (3 ms pulse duration) of light to neurons under current-clamp recording mode. Remarkably, nerve impulses elicited with 980-nm NIR illumination were comparable to those elicited with 470-nm light (Fig. 4c), indicating a sufficient blue luminescence from the UCNPs to activate ChR2 and drive neuronal depolarization beyond the nerve impulse firing threshold. Moreover, 980-nm illumination of the ChR2-expressing neurons cultured on the hybrid scaffolds enabled the generation of time-locked, sustained naturalistic trains of impulses with millisecond-timescale temporal resolution, in response to light pulses delivered at 1 Hz, 5 Hz and 10 Hz (Fig. 4d). Impulses were generated with frequencies up to 20 Hz using NIR light (Fig. S11 in ESI). This is in contrast to 980-nm illumination of control substrates, i.e. ChR2-infected neurons on PLGA substrates (Fig. S12 in ESI) and non-infected neurons on PLGA-UCNP substrates (Fig. S13 in ESI), which showed negligible membrane depolarization and a lack of nerve impulse generation. This indicates the inability of 980-nm NIR light alone to activate ChR2-expressing neurons. The membrane depolarization and the reliable generation of action potentials described above was obtained for polymer films containing a minimal UCNP concentration of 8.3 μg/mm^2, wherein lower concentrations did not generate action potentials.

The physicochemical properties of the upconversion nanomaterial can play a significant role in determining the overall effectiveness of our approach. For instance, we had initially considered employing upconversion nanomaterials in the form of nanorods, due to closer resemblance to bulk materials.[18] These upconversion nanorods (UCNRs) were synthesized as reported previously,[18] using the Yb^{3+}/Tm^{3+} dopants to achieve a blue luminescence spectra similar to the core-shell UCNPs shown in Figure 2 (Fig. S14 in ESI). These rod-shaped particles, with a length of about 200 nm and width of 50 nm, were embedded within PLGA films and cultured with neurons (Fig. S15 in ESI). However, the whole-cell patch clamping experiments showed inconsistent and unreliable nerve impulse generation, especially at higher frequency pulses (Fig. S16 in ESI). In addition, nerve impulse generation with the UCNR-based hybrid scaffolds required higher NIR power (2 W) and

Author Manuscript Author Manuscript Author Manuscript Author Manuscript

longer NIR pulse durations (50 ms) compared to the core-shell UCNP-based hybrid scaffolds (1 W, 3 ms). In fact, core-shell UCNP-based hybrid scaffolds enabled successful generation of action potentials at longer NIR pulse duration as well, in the form of sustained spikelets (Fig. S17 in ESI). The ineffectiveness of UCNRs can be attributed to multiple factors, including non-uniformity and random orientation after film formation (Fig. S18 in ESI), as well as surface-quenching effects from the lack of an inert shell (complete shell formation on UCNRs is a technical challenge due to highly anisotropic particle growth[34]). Besides, the larger size and rod-like morphology of UCNRs makes them less favorable when considering future applications for *in vivo* studies.[35] In this way, the design and systematic testing of nanomaterials is invaluable for evaluating their prospects in neural applications such as optogenetics.

In summary, we have developed a novel and promising proof-of-concept/method as a complementary technique to expand the optogenetic toolbox. Our approach is unique in that we employ UCNPs as mediators to convert NIR light into opsin-activating visible light. From an application perspective, UCNPs can be excited with relatively inexpensive continuous wave (CW) diode lasers; this is in stark contrast to two-photon approaches, which require high-energy femtosecond pulsed lasers and instrumentation for raster scanning of a focused beam over the region of interest.[36] Moreover, while conventional approaches focus on engineering new opsin-variants to impart red-shifted spectral sensitivity,[37, 38] our approach entailed synthetically-tuning UCNPs to emit at a specific wavelength of light (e.g. 475 nm blue light) upon NIR excitation to activate ChR2. In this way, our current *in vitro* approach can be useful to assess the UCNP-mediated stimulation of a variety of different opsins, which exhibit peak sensitivity to different wavelengths of light (e.g. green, yellow) and can be excitatory or inhibitory.[9] In other words, a library of combinatorial UCNPs can be systematically designed and easily tested for stimulating a corresponding library of well-established opsins. This offers an additional wavelength for optogenetic control, which can facilitate multiplexed stimulation and spatiotemporally confine emission to regions containing UCNPs. Such a level of control can help explore specific biological questions at the single-cell level on these unique neural-material interfaces, which are not only biocompatible but also provide a biologically-relevant functionality. With rising interest in improving control over neuronal activity and function, creating effective interfaces between neurons and external materials will be invaluable. Overall, the integration of chemical control and nanotechnology with optogenetics holds great potential for advancing applications in neuroscience research.

Supplementary Material

Refer to Web version on PubMed Central for supplementary material.

Acknowledgments

K.-B. Lee acknowledges financial support from the National Institute of Health (NIH) Director's New Innovator Award [1DP20D006462-01], National Institute of Neurological Disorders and Stroke (NINDS) of the NIH [1R21NS085569-02], N.J. Commission on Spinal Cord grant [CSR13ERG005] and the Rutgers IAMDN. Z.P. Pang acknowledges financial support from National Institute on Drug Abuse (NIDA) R21 DA035594, Sinsheimer Scholar Award and Robert Wood Johnson Foundation. We would like to thank Benjamin Deibert for help with PXRD.

Author Manuscript Author Manuscript Author Manuscript Author Manuscript

References

1. Alivisatos AP, Andrews AM, Boyden ES, Chun M, Church GM, Deisseroth K, Donoghue JP, Fraser SE, Lippincott-Schwartz J, Looger LL, Masmanidis S, McEuen PL, Nurmikko AV, Park H, Peterka DS, Reid C, Roukes ML, Scherer A, Schnitzer M, Sejnowski TJ, Shepard KL, Tsao D, Turrigiano G, Weiss PS, Xu C, Yuste R, Zhuang X. ACS Nano. 2013; 7:1850–1866. [PubMed: 23514423]
2. Boyden ES, Zhang F, Bamberg E, Nagel G, Deisseroth K. Nat Neurosci. 2005; 8:1263–1268. [PubMed: 16116447]
3. Zhang F, Gradinaru V, Adamantidis AR, Durand R, Airan RD, de Lecea L, Deisseroth K. Nat Protoc. 2010; 5:439–456. [PubMed: 20203662]
4. Tye KM, Deisseroth K. Nat Rev Neurosci. 2012; 13:251–266. [PubMed: 22430017]
5. Brieke C, Rohrbach F, Gottschalk A, Mayer G, Heckel A. Angew Chem Int Ed. 2012; 51:8446–8476.
6. Chuong AS, Miri ML, Busskamp V, Matthews GA, Acker LC, Sorensen AT, Young A, Klapoetke NC, Henninger MA, Kodandaramaiah SB, Ogawa M, Ramanlal SB, Bandler RC, Allen BD, Forest CR, Chow BY, Han X, Lin Y, Tye KM, Roska B, Cardin JA, Boyden ES. Nat Neurosci. 2014; 17:1123–1129. [PubMed: 24997763]
7. Lin JY, Knutsen PM, Muller A, Kleinfeld D, Tsien RY. Nat Neurosci. 2013; 16:1499–1508. [PubMed: 23995068]
8. Klapoetke NC, Murata Y, Kim SS, Pulver SR, Birdsey-Benson A, Cho YK, Morimoto TK, Chuong AS, Carpenter EJ, Tian Z, Wang J, Xie Y, Yan Z, Zhang Y, Chow BY, Surek B, Melkonian M, Jayaraman V, Constantine-Paton M, Wong GK, Boyden ES. Nat Methods. 2014; 11:338–346. [PubMed: 24509633]
9. Yizhar O, Fenno LE, Davidson TJ, Mogri M, Deisseroth K. Neuron. 2011; 71:9–34. [PubMed: 21745635]
10. Wang F, Liu XG. Chem Soc Rev. 2009; 38:976–989. [PubMed: 19421576]
11. Gu Z, Yan L, Tian G, Li S, Chai Z, Zhao Y. Adv Mater. 2013; 25:3758–3779. [PubMed: 23813588]
12. Chen G, Qiu H, Prasad PN, Chen X. Chem Rev. 2014; 114:5161–5214. [PubMed: 24605868]
13. Chien YH, Chou YL, Wang SW, Hung ST, Liau MC, Chao YJ, Su CH, Yeh CS. ACS Nano. 2013; 7:8516–8528. [PubMed: 24070408]
14. Ni D, Zhang J, Bu W, Xing H, Han F, Xiao Q, Yao Z, Chen F, He Q, Liu J, Zhang S, Fan W, Zhou L, Peng W, Shi J. ACS Nano. 2014; 8:1231–1242. [PubMed: 24397730]
15. Wang F, Banerjee D, Liu Y, Chen X, Liu X. Analyst. 2010; 135:1839–1854. [PubMed: 20485777]
16. Zhang F, Vierock J, Yizhar O, Fenno LE, Tsunoda S, Kianianmomeni A, Prigge M, Berndt A, Cushman J, Polle J, Magnuson J, Hegemann P, Deisseroth K. Cell. 2011; 147:1446–1457. [PubMed: 22196724]
17. Nagel G, Szellas T, Huhn W, Kateriya S, Adeishvili N, Berthold P, Ollig D, Hegemann P, Bamberg E. Proc Natl Acad Sci USA. 2003; 100:13940–13945. [PubMed: 14615590]
18. Wang F, Han Y, Lim CS, Lu YH, Wang J, Xu J, Chen HY, Zhang C, Hong MH, Liu XG. Nature. 2010; 463:1061–1065. [PubMed: 20182508]
19. Wang F, Liu XG. J Am Chem Soc. 2008; 130:5642–5643. [PubMed: 18393419]
20. Yi GS, Chow GM. Adv Funct Mater. 2006; 16:2324–2329.
21. Lin JY, Lin MZ, Steinbach P, Tsien RY. Biophys J. 2009; 96:1803–1814. [PubMed: 19254539]
22. Li Z, Zhang Y. Nanotechnology. 2008; 19:345606. [PubMed: 21730655]
23. Bogdan N, Vetrone F, Ozin GA, Capobianco JA. Nano Lett. 2011; 11:835–840. [PubMed: 21244089]
24. Wang F, Wang J, Liu X. Angew Chem Int Ed. 2010; 49:7456–7460.
25. Zhang F, Che R, Li X, Yao C, Yang J, Shen D, Hu P, Li W, Zhao D. Nano Lett. 2012; 12:2852–2858. [PubMed: 22545710]
26. Deng R, Qin F, Chen R, Huang W, Hong M, Liu X. Nat Nano. 2015; 10:237–242.
27. Liu H, Xu CT, Lindgren D, Xie H, Thomas D, Gundlach C, Andersson-Engels S. Nanoscale. 2013; 5:4770–4775. [PubMed: 23604490]

Author Manuscript Author Manuscript Author Manuscript Author Manuscript

28. Xu CT, Svenmarker P, Liu H, Wu X, Messing ME, Wallenberg LR, Andersson-Engels S. ACS Nano. 2012; 6:4788–4795. [PubMed: 22568960]
29. Orive G, Anitua E, Pedraz JL, Emerich DF. Nat Rev Neurosci. 2009; 10:682–692. [PubMed: 19654582]
30. Danhier F, Ansorena E, Silva JM, Coco R, Le Breton A, Préat V. J Controlled Release. 2012; 161:505–522.
31. Bible E, Chau DYS, Alexander MR, Price J, Shakesheff KM, Modo M. Biomaterials. 2009; 30:2985–2994. [PubMed: 19278723]
32. Karmazinova M, Lacinova L. Physiol Res. 2010; 59:S1–7. [PubMed: 20626213]
33. Bean BP. Nat Rev Neurosci. 2007; 8:451–465. [PubMed: 17514198]
34. Zhang C, Lee JY. ACS Nano. 2013; 7:4393–4402. [PubMed: 23570424]
35. Geng Y, Dalhaimer P, Cai S, Tsai R, Tewari M, Minko T, Discher DE. Nat Nano. 2007; 2:249–255.
36. Park YI, Lee KT, Suh YD, Hyeon T. Chem Soc Rev. 2015; 44:1302–1317. [PubMed: 25042637]
37. Packer AM, Peterka DS, Hirtz JJ, Prakash R, Deisseroth K, Yuste R. Nat Methods. 2012; 9:1202–1205. [PubMed: 23142873]
38. Prakash R, Yizhar O, Grewe B, Ramakrishnan C, Wang N, Goshen I, Packer AM, Peterka DS, Yuste R, Schnitzer MJ, Deisseroth K. Nat Methods. 2012; 9:1171–1179. [PubMed: 23169303]

Author Manuscript Author Manuscript Author Manuscript Author Manuscript

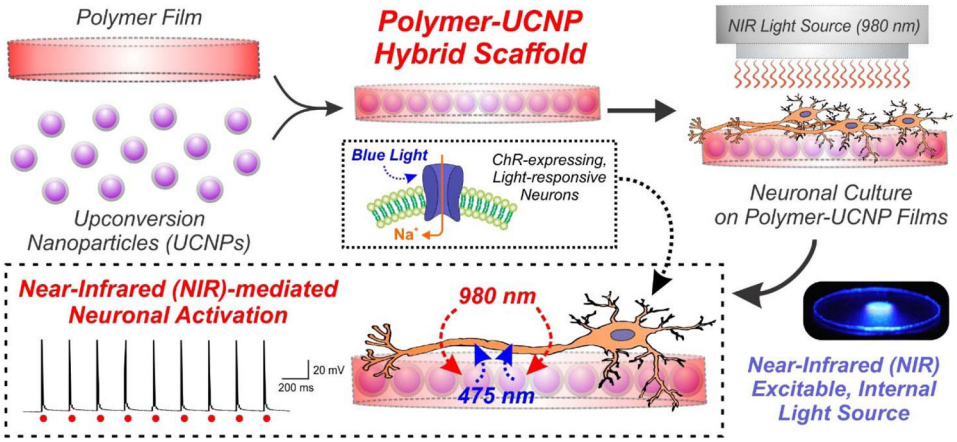

Figure 1. Schematic diagram depicting the generation and application of polymer-UCNP hybrid scaffolds for optogenetic neuronal activation

Upconversion nanoparticles (UCNPs) were embedded within polymeric films to form biocompatible hybrid scaffolds for neuronal culture. The UCNPs served as internally excitable light sources that convert NIR light into blue light, thus facilitating optogenetic activation of channelrhodopsin (ChR)-expressing neurons.

Author Manuscript Author Manuscript Author Manuscript Author Manuscript

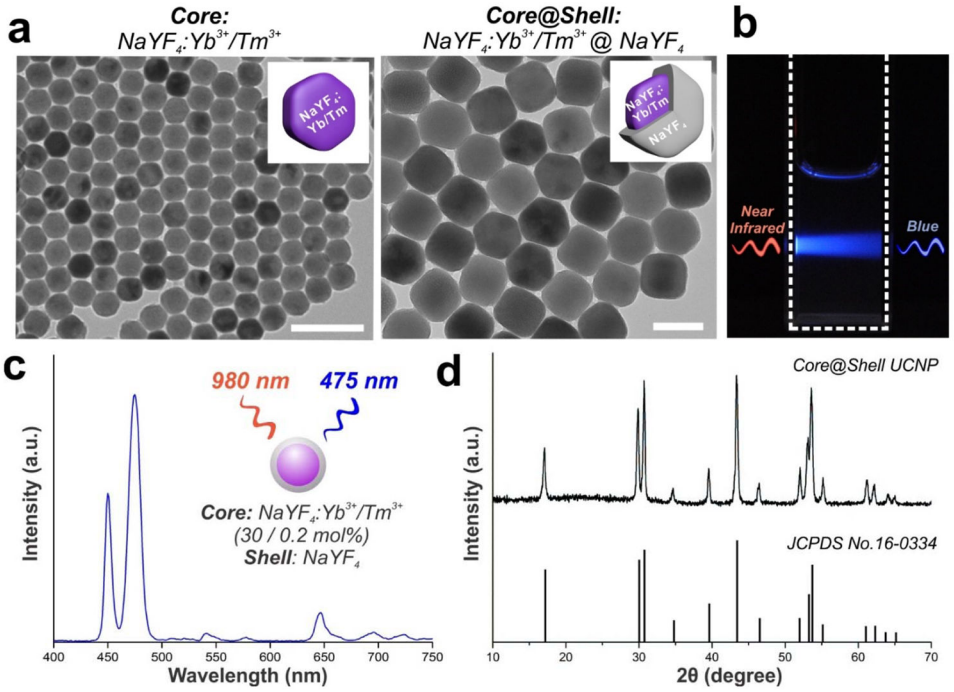

Figure 2. Monodisperse core-shell UCNPs with blue emission upon near-infrared excitation were synthesized

(a) Transmission electron microscopy (TEM) image of core $NaYF_4$:Yb^{3+}/Tm^{3+} (30 / 0.2 mol%) nanoparticles (*left*, scale bar: 100 nm) and core@shell $NaYF_4$:Yb^{3+}/Tm^{3+} (30 / 0.2 mol%)@$NaYF_4$ UCNPs (*right*, scale bar: 50 nm). (b) Photographic image of a cuvette with a suspension of UCNPs under laser excitation at 980-nm. (c) Upconversion emission spectrum of core-shell UCNPs in hexane solution (1 mg/mL) under near-infrared light excitation at 980-nm. (d) Powder X-ray diffraction (PXRD) patterns of the core-shell UCNPs, showing all peaks to be well-indexed in accordance with the β-hexagonal-phase $NaYF_4$ crystal structure (Joint Committee on Powder Diffraction Standards file No. 16-0334).

Author Manuscript Author Manuscript Author Manuscript Author Manuscript

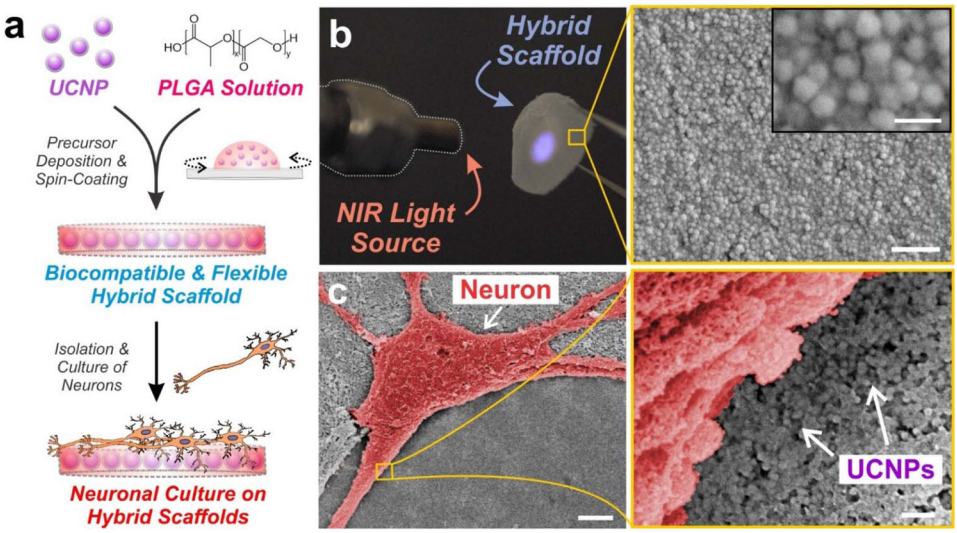

Figure 3. Blue-emitting UCNPs were embedded within thin polymer films of PLGA and cultured with hippocampal neurons

(a) Schematic depicting preparation of poly(lactic-co-glycolic acid) (PLGA)-embedded UCNP hybrid scaffolds for hippocampal neuronal cultures. (b) Photographic image of the flexible hybrid scaffold film. The blue luminescence under 980-nm laser excitation illustrates the encapsulation of UCNPs throughout the PLGA film. Scanning electron microscopy (SEM) image shows the distribution of the UCNPs within the PLGA film. Scale bar: 500 nm (*bottom*), 100 nm (*inset*). (c) Scanning electron microscopy (SEM) image of a hippocampal neuron (pseudo-colored *red* for contrast) cultured on the polymer-UCNP hybrid scaffolds at 14 DIV. Scale bar: 5 μm (*left*), 200 nm (*right*).

Author Manuscript Author Manuscript Author Manuscript Author Manuscript

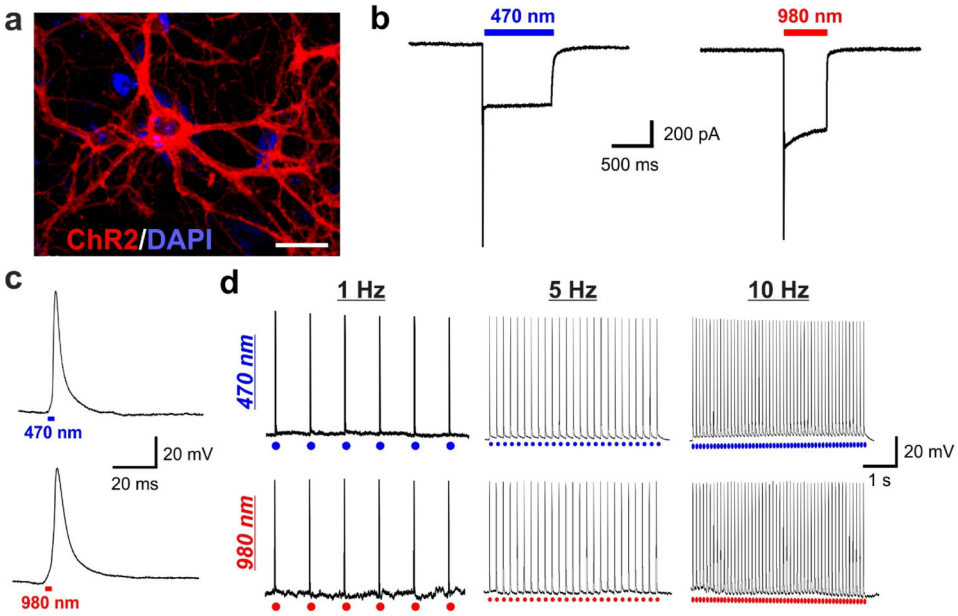

Figure 4. Channelrhodopsin-expressing neurons grown on polymer-UCNP films exhibit robust excitatory activation upon NIR-light illumination, comparable to blue LED illumination

(a) Hippocampal neurons expressing ChR2-tdTomato (*red*). Scale bar: 50 μm. (b) Representative traces of inward current flow in voltage-clamped neuron evoked by 470-nm light (5 mW) and 980-nm light (1 W). (c) Magnified action potential induced by 470-nm light (*top*) and 980-nm light (*bottom*). (d) Representative traces showing repetitive action potentials in a current-clamped hippocampal neuron evoked by 1 Hz, 5 Hz and 10 Hz train of light pulses from 470-nm light (*top*; 250 mW, 3 ms pulse width) and 980-nm light (*bottom*; 1 W, 3 ms pulse width).